



Application of CO atmosphere in the liquid phase synthesis as a universal way to control the microstructure and electrochemical performance of Pt/C electrocatalysts



Anastasia A. Alekseenko, Evgenia A. Ashihina, Svetlana P. Shpanko, Vadim A. Volochaev, Olga I. Safronenko, Vladimir E. Guterman*

Southern Federal University, Chemistry Faculty, 7 Zorge st., Rostov-on-Don, 344090, Russia

ARTICLE INFO

Keywords:

Platinum nanoparticles
Size effect
Pt/C electrocatalyst
Oxygen reduction reaction
CO chemisorption

ABSTRACT

A number of new platinum-based catalysts with Pt loading from 15.2% to 17.3% was obtained by wet chemical synthesis. Ethylene glycol, formaldehyde, and formic acid were used as reducing agents. The synthesis was performed both at ambient conditions and when the solution was saturated with carbon monoxide.

It was shown that the catalysts obtained in the CO environment possess a larger electrochemical active surface area (ECSA), $140\text{--}146\text{ m}^2\text{ g}^{-1}$ (Pt), compared to the analogues that have been made at ambient conditions, $72\text{--}120\text{ m}^2\text{ g}^{-1}$ (Pt). This could be explained by a smaller platinum NPs average size as well as a very narrow distribution of their size. In contrast to the materials synthesized at ambient conditions, the ECSA values of the catalysts, obtained in the CO-saturated media, in fact, do not depend on the type of reducing agent and the synthesis conditions. Such catalysts demonstrate the best mass-activity in ORR, which is higher than that of the commercial Pt/C catalyst HISPEC 3000 (20% of Pt loading) and the analogues obtained at ambient conditions.

Distinctive features of the nanoparticles nucleation/growth and their structure were determined and studied when formic acid was applied as a reducing agent. Absorption processes of the CO molecules on the surface of platinum nuclei are a plausible explanation for the CO influence on nucleation/growth and, therefore, on the microstructure and ECSA, as well as other functional characteristics of Pt/C-catalysts.

1. Introduction

Proton exchange membrane fuel cells (PEMFC) are one of the most efficient and nature-friendly energy sources with respect to direct transformation of fuel energy into electrical energy [1–5]. Proper electrocatalysts for PEMFC industry are very important due to their significant influence on reactions rate [1–5]. At present great attention is focused on parameters of a cathode catalyst in which oxygen electro-reduction reactions (ORR) are taking place. The reason is that the ORR rate is lower compared to that of the hydrogen electro-oxidation reaction, therefore polarization of the cathode is higher. At the same time, the ORR intermediate substances intensify corrosion of the cathode components in the process of PEMFC exploitation [1,2].

Electrocatalysts designed for PEMFC application should possess such characteristics as high surface area, good electrical conductivity, high resistance to contaminations, as well as reasonable price [3–6]. Catalyst mass activity and high stability (ability to be active during a long period of time) are the most important parameters among

electrocatalyst properties. Pure platinum nanoparticles (NPs) and Pt-based NPs, typically distributed on developed carbon support, at present are the best system among those available on the market [3,4,6]. Informative reviews [5–8] are dedicated to a huge number of publications which deal with a synthesis of electrocatalysts. Nevertheless, optimization of the hierarchically organized micro-nanostructure of Pt-contained electrocatalysts is still an extremely urgent task for renewable energy industry worldwide, stipulated by the need to increase both mass activity and stability of the catalysts [3–6,8,9].

The platinum surface in Pt/C catalyst, available for adsorption and electrochemical transformation of the reacting particles, is heterogeneous. Different types of facets, edges, steps and vertices on the NPs surface have different specific (per unit of surface) activity in ORR [3,5,10]. NPs activity and, hence, their facets activity typically decrease with the decrease in the NPs size. To the best of our knowledge this is the most common point of view among the experts working on catalysts development [2,5,8,11–13]. Assuming that the entire electrochemically active surface area of platinum (ECSA) is an aggregate including parts

* Corresponding author.

E-mail addresses: gut57@mail.ru, guter@sfedu.ru (V.E. Guterman).

of the surface with the determined specific activity (for each type), the relationship between mass activity of the catalyst (J_{mass}) and its ECSA can be described by Eq. (1) [14]:

$$J_{mass} = \sum (J_{sp}^i \Theta_i) ECSA \quad (1)$$

where J_{sp}^i - is specific activity of each type of catalytically active parts of the NPs surface; Θ_i - is the surface part of platinum NPs, related to i -type of facets or edges, or vertices which could depend on the size and the shape of NPs [14,15].

Various approaches to increase Pt/C mass activity in ORR are based on the attempt to increase the ECSA, the proportion of active sites on the surface of NP platinum (Θ_i) and/or specific activity (J_{sp}^i) without changing or even reducing the loading of the precious metal in the catalyst.

Doping of platinum with some d-metals, including formation of nanoparticles with the primary or secondary M-core and Pt-shell architecture, seems to be a logical and effective way to increase J_{sp}^i [2–4,6,11,16–19]. Unfortunately, selective dissolution of the alloying component, which might occur in the process of the catalyst functioning, leads to contamination of the polymer membrane and decreases its proton conductivity [20].

An increase in the proportion of the active regions of surface - Θ_i can be achieved by optimizing the shape of platinum nanocrystals [5–7,10,17] and increasing the ECSA by decreasing the size of the nanoparticles. Taking into account the antisymbiotic character of changes in J_{sp}^i and ECSA during the changes in the size of the nanoparticles [11], as well as the possible transformation in the shape of nanocrystals during the catalyst operation [5], it should be noted that obtaining materials with the optimal structure is a very complicated task.

Although we omit discussing the mechanisms of platinum-carbon materials degradation [5,6,8,13,14,20], we would like to mention that the narrow size distribution of the nanoparticles, as well as the uniformity of their distribution over the carrier surface (spatial distribution), are essential requirements for increasing not only mass activity but also stability of the catalyst [3,8,15].

The methods to control the microstructure of Pt/C catalysts are rather diverse. Under the reduction conditions of the platinum precursors in the liquid phase the kind and concentration of precursor [21], the type and concentration of the reducing agent [22–24], the temperature [23], pH [22], the composition and nature of the solvent components [22–26] have an influence on the nucleation/growth processes of the nanoparticles. Interesting results of the platinum NPs synthesis were obtained while using the so-called colloidal methods, when the adsorption of surfactant molecules, introduced into the solution on the surface of platinum particles, hindered their growth leading to the size decrease and narrowing of dispersion in the size distribution [27–29]. Growing platinum NPs in emulsion droplets (the case when they play the role of a nanoreactor) makes it possible to obtain Pt/C catalysts with a narrow size distribution [30]. Unfortunately, the addition of surfactants to the solution leads to contamination of the carbon carrier surface and requires subsequent, sometimes very complicated, catalyst purification. For example, an application of the Bönnemann method [27,28] involves the stage of thermal treatment of the resulting material in the inert atmosphere at 300 °C. This is done to remove the stabilizing agent. During this sort of post-treatment, platinum nanoparticles may coalesce, causing the decrease in the active platinum surface area.

While discussing non-polluting methods of the influence on the formation of platinum NPs during the synthesis in the liquid phase, it is worth mentioning the paper [31], in which the authors demonstrated the ability to control dimensional distribution of platinum nanoparticles, formed in the polyol synthesis by the UV irradiation of the reaction mixture. Suspensions containing nanoparticles with the size distribution from 1 nm to 5.8 nm and with high stability (at the maximum nanoparticle size) were obtained.

Interesting synthetic approaches associated with the introduction of CO molecules into the system were used in the preparation of gold nanoclusters [32], platinum nanotubes, spherical palladium nanoparticles and gold nanowires [33]. Solvothermal synthesis was also used to obtain platinum-nickel nanoparticles of variable composition but of a constant size [34]. All the above-mentioned syntheses were carried out at elevated temperatures, in solutions of complex composition [32,33], at elevated pressure [34]. The authors [32,33] associated the positive effect of carbon monoxide with the size and shape of the nanoparticles, formed with the participation of CO molecules in the oxidation-reduction reaction, while Strasser et al. [34] pointed out the decisive role of the size-dependent CO surface chemisorption and reversible Ni-carbonyl formation as the key factors to achieve constant particle size (4 nm) and temperature controlled Ni content in PtNi nanoparticles.

In an attempt to continue previous studies [32–34], we hypothesized the effect of CO molecules on the nucleation/growth of platinum NPs during the chemical reduction of Pt (IV) in the solution of formaldehyde at a comparatively low temperature [35,36]. It was found that strong chemisorption of CO molecules on the surface of the growing platinum clusters hindered the growth of nanoparticles and lead to the decrease in their size. As a result, Pt/C catalysts were obtained with a very narrow dispersion of the size and spatial distribution of nanoparticles. High values of the electrochemically active surface of platinum ECSA (140–150 m² g⁻¹ of Pt) were achieved. At the same time, CO molecules adsorbed on the surface of platinum and carbon were easily desorbed while synthesized materials were dried at 80–100 °C and they did not exert any influence on the electrochemical behavior of Pt/C catalysts [36].

The purpose of this paper is to study CO application as a regulator of the platinum NPs nucleation/growth while using a wide range of simple and "soft" liquid-phase synthesis methods. We try to get an answer to the question whether CO is a unique agent capable of making a real impact on the formation of Pt/C in various liquid-phase systems, and also to assess to what extent such influence depends on the composition of the media or synthesis conditions.

2. Experimental

The Pt/C catalysts were synthesized via chemical reduction of H₂PtCl₆·6H₂O with three kinds of reducing agents: formaldehyde, ethylene glycol, and formic acid. Vulcan XC-72 (Cabot Corp., S_{BET} = 250–280 m² g⁻¹) was used as a support. The synthesis was carried out both in ambient atmosphere and in a solution, saturated with CO. The calculated mass fraction of platinum in Pt/C was 20%.

2.1. Synthesis methods

2.1.1. Formaldehyde as a reducing agent

At first 0.1 g of Vulcan XC-72 carbon powder was suspended in 10 ml of ethylene glycol with the appropriate amount of chloroplatinic acid. Then 1.0 ml of 37% formaldehyde was added to the suspension. Thereafter, 1 M NaOH solution (H₂O:EG 1:1) was gradually added to the suspended mixture until the pH of the mixed solution reached 11–12. Then, the suspension was maintained for 2 h, heated at 90 °C at constant stirring. Finally, a strong electrolyte such as 1 M NaCl solution was added as a sedimentation promoter. Half an hour later, the catalysts were filtered, washed several times with water and ethanol, and then dried.

2.1.2. Ethylene glycol as a reducing agent

10 ml of 8% isopropanol solution in water, 0.1 g of Vulcan-72, the calculated amount of chloroplatinic acid and 60 ml of ethylene glycol were mixed under stirring in a flask. An ultrasonic homogenization was applied to the suspension and pH of the solution was corrected to the value 6, using 1 M NaOH solution (H₂O:EG 1:1). The synthesis was

carried out for 2 h at 80 °C under intensive stirring, after that the suspension was kept for 0.5 h without any heating at room temperature. After filtration, the product was washed many times with water and ethanol, and then it was dried.

2.1.3. Formic acid as a reducing agent

0.1 g of carbon was mixed with 25 ml of 0.1 M HCOOH and 10 ml of ethylene glycol. The calculated amount of $H_2[PtCl_6] \cdot 6H_2O$ was added after an ultrasonic homogenization of the suspension. The synthesis was carried out for 0.5 h at 90 °C and then 0.5 h without any heating under stirring. The obtained powder was filtered and washed several times with water and ethanol, then dried for 2 h at 80 °C. Pt-loading in Pt/C catalysts was determined by thermogravimetric analysis after 40 min of calcination at 800 °C. To study the influence of carbon monoxide on the microstructure and electrochemical properties of Pt/C catalysts, solution saturated with CO was applied at the chemical reactor. CO, injected into the solution, was obtained by decomposition of formic acid under the influence of hot concentrated sulfuric acid.

Next, the obtained materials were marked depending on the type of the atmosphere and the reducing agent used: air atmosphere – F (formaldehyde), E (ethylene glycol), FA (formic acid); CO atmosphere – F_{CO} , E_{CO} , FA_{CO} , correspondingly. The synthesis of the samples, performed according to the technique described above, was repeated at least three times, which allowed us to evaluate the reproducibility of characteristics of the obtained Pt/C materials.

In order to determine whether CO molecules can react as a reducing agent with respect to Pt (IV) in liquid-phase synthesis processes, CO was passed through a carbon suspension (Vulcan XC72) in water solutions of $H_2[PtCl_6] \cdot 6H_2O$ and mixture of $H_2[PtCl_6] \cdot 6H_2O$ with NaOH (pH = 11) at 90 °C for 30 min. The amount of the precursor was chosen based on a 20% platinum content in the final Pt/C product in the case of a complete reduction of the precursor. Then, we extracted, washed and dried the obtained material according to standard procedures. According to the results of thermogravimetry, the presence of platinum in the obtained material was not established. Consequently, at a temperature of about 90 °C, CO practically does not participate in the reduction of the platinum precursor.

2.2. Powder X-ray diffraction measurements

The powder X-ray diffraction data were collected on automatic diffractometer ARL X'TRA with a copper anode, $K\alpha$ -radiation ($<\lambda> = 1.5418 \text{ \AA}$) in the range of 2Θ from 10° to 90°, the step size was 0.02° and 0.08°. Typical settings: 40 kV, 30 mA, scan rate from 8 to 0.5° per minute depending on the type of measurements. $K\beta$ and fluorescent radiation were filtered by Si(Li) - a solid state detector. Polycrystalline α -quartz was used as a calibration standard. To collect the diffraction data we used the ThermoScientific© WinXRD program, for full-profile analysis - the WinPlotr package(Fullprof), for general data processing- SciDavis.

The average diameter of crystallites (D_{av}) was calculated according to the Scherer equation, this procedure being described earlier in [37].

2.3. Transmission electron microscopy (TEM)

The TEM study was performed using a JEM-2100 (JEOL, Japan) microscope operated at 200 kV. 0.5 mg of electrocatalyst powder was placed in 1 ml of heptane to prepare the samples for the TEM analysis. Then, the suspension was ultrasonically dispersed and one drop of suspension was deposited onto a copper grid sputter-coated with carbon. The metal particle size distribution and the average size of the nanoparticles (D_{NP}) in the catalysts were obtained by direct measurement of 500 randomly selected particles by the TEM images.

2.4. Electrochemical measurements

The electrochemical active surface area (ECSA) was determined by cyclic voltammetry (CV), no rotation was applied to an electrode. The main electrode consisted of a glassy-carbon part, integrated into a teflon cylinder. The catalysts under study were injected as “catalyst inks” and they formed a thin layer on the top of the glassy-carbon part. As a second electrode, a platinum wire was mounted. A silver–silver chloride electrode was used as a reference electrode at the setup.

First of all, in order to perform standardization of the electrode surface, 100 cycles were recorded in the range of potentials from 0.037 to 1.2 V at the speed 200 mV s^{-1} . Then two CV-curves were obtained at the sweep rate of 20 mV s^{-1} . The ECSA was calculated according to the amount of electricity spent on electrochemical adsorption/desorption of atomic hydrogen at the second cycle, as described in [35].

Catalyst activity in oxygen reduction reaction (ORR) was measured in the sweep potential range from 0.04 to 1.20 V. The electrolyte (0.1 M $HClO_4$) was saturated with oxygen for 40 min, then linear voltammograms were measured at rotation speed equal to 400, 900, 1600 and 2500 rpm.

These curves were normalized in accordance with [38]. The cell voltage, E , is defined as: $E = E_{reg} - J_i^*R$, where: E_{reg} – is a registered value of potential, J_i^*R – is the ion conduction resistance. Compensation for the resistance of the electrolyte was applied to $R = 26 \text{ ohm}$. This value well corresponded to [11,38,39]. Correction of RDE LSVs curves, depicting the contribution of the processes in oxygen-free (Ar) solution ($J_i(O_2) - J_i(Ar)$) was made as written in [36]. The electrocatalytic activities of Pt/C catalysts in ORR (kinetic currents) were extracted from the normalized RDE LSVs using a well-known mass-transport correction for RDE measurements [11,40], resulting from the Koutecky-Levich equation:

$$J_k = J_d J / (J_d - J),$$

where J - is current, experimentally obtained at $E = 0.90 \text{ V}$, J_d - refers to the measured diffusion-limited current, and J_k - is the mass-transport free kinetic current.

The number of electrons, involved in ORR was determined by the slope of the line in coordinates $1/i - 1/\omega^{-0.5}$, according to [40].

An electrochemical performance of the synthesized Pt/C samples was compared to the performance of commercial HiSPEC-3000 catalyst, which contained 20% wt. of platinum.

3. Results and discussion

The mass fraction of platinum ($\omega(\text{Pt})\%$) for the obtained samples was a little bit less than it was expected according to preliminary calculations before the synthesis (Table 1). The exact value depended both on the reduction agent and the atmosphere conditions. The lowest platinum content (15.2–15.3%) was found in FA and FA_{CO} samples, where formic acid was used as a reducing agent. In this case there is

Table 1

Dependence of $\omega(\text{Pt})$ and D_{av} values for materials with different synthesis route on the solvent used and the atmosphere composition (air or carbon monoxide).

Catalyst	$\omega(\text{Pt})$, wt.%	D_{av} , nm ^a
EG	17 ± 0.5	1.6
EG_{CO}	16.1 ± 0.5	1.1
F	17.3 ± 0.5	2.1
F_{CO}	15.5 ± 0.5	1.0
FA	15.3 ± 0.5	4.2
FA_{CO}	15.2 ± 0.5	1.3
HiSPEC 3000	20 ± 0.6	3.2

Boldface indicates the parameters measured for catalysts that are synthesized in a CO atmosphere.

^a A typical deviation for the average diameter of crystallites is $\pm 5\%$.

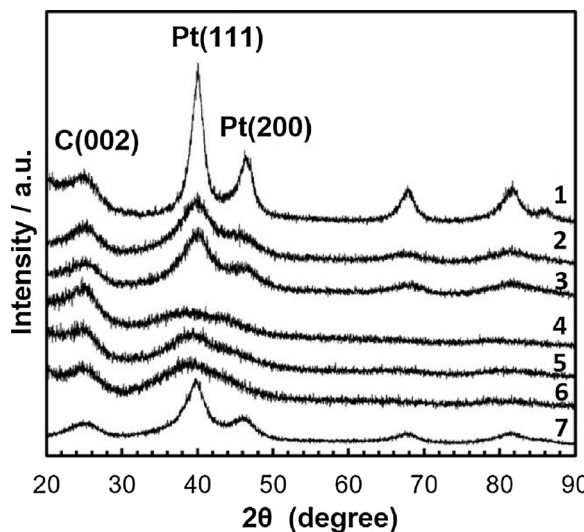


Fig. 1. Powder X-ray diffraction patterns of Pt/C samples obtained with FA (1, 2), F (3, 4), EG (5, 6) as a reducing agent in ambient conditions (1, 3, 5) and in CO-atmosphere (2, 4, 6), as well as the commercial Pt/C catalyst HiSPEC 3000 (7).

almost no CO influence on $\omega(\text{Pt})$.

Replacement of the air atmosphere (ambient conditions) with the CO environment under conditions of polyol and formaldehyde synthesis leads to the decrease in $\omega(\text{Pt})$ from 17.3% and 17% to 15.5% and 16.1%, respectively (Table 1). The discrepancy between the calculated and the actual mass proportions of platinum in Pt/C materials obtained in the presence of an excess of a reducing agent in the liquid phase is usually due to the incomplete sorption of nanoparticles formed in the liquid phase by the surface of the carbon carrier [23]. Apparently, adsorption of CO molecules on the surface of platinum nanoparticles sometimes hinders not only their growth, but also adsorption on the surface of the particles of the carbon carrier.

Powder diffractograms of the synthesized Pt/C catalysts contain reflections of semi-amorphous graphite (002) and platinum (111), (200), (220) and (311). The most distinct lines to identify platinum are the reflections with indices (111) and (200). The region of the diffractograms, where (111) and (200) reflections data are located, is shown in Fig. 1. For materials synthesized in the CO-saturated solvent, broadening of these reflections is observed (Fig. 1), thus indicating the decrease in the size of crystallites (Table 1).

D_{NP} of Pt NPs, obtained during the synthesis at ambient conditions, decreases in the FA > F > EG series from 4.2 to 1.6 nm. The presence of CO molecules in the reaction medium during the reduction of Pt (IV) leads to the formation of crystallites whose average size is practically independent of the type of the reducing agent (Table 1). The effect of CO is the most pronounced for the material obtained with formic acid used as a reducing agent: D_{NP} in this case decreases from 4.2 nm to ~ 1.3 nm.

The data of the electron microscopic study of selective materials (Fig. 2) correlate well with the results of X-ray diffraction (Table 1). The minimum size of nanoparticles (~ 1.8 nm) among the studied materials and the narrowest size distribution is demonstrated by the EG_{CO} catalyst. The average size of the NPs in FA_{CO} catalyst is about 2 nm, and in the FA it is 4.3 nm. A significant coalescence of nanoparticles is observed in the FA sample and is very weakly expressed in the FA_{CO} and EG_{CO} catalysts. The samples obtained in the CO-saturated solvent (CO atmosphere) are characterized by a more uniform spatial distribution of the platinum nanoparticles. It should be noted that a slight difference in the dimensions of nanoparticles, determined by the XRD and TEM methods, is rather typical for the same sort of materials [22,41].

ECSA is one of the most important characteristics of a catalyst; it was calculated by the hydrogen region of CVs, recorded after

standardization of the sample surface (see Experimental section) (Fig. 3A–C). As expected, the area of the active surface of platinum correlates well with the average diameter of the crystallites increasing as D_{Av} decreases in the series FA < $\text{HiSPEC} \leq \text{F} \approx \text{EG} < \text{FA}_{\text{CO}} \leq \text{EG}_{\text{CO}} \approx \text{F}_{\text{CO}}$ (Fig. 3).

Accordingly, the ECSA of the catalysts, obtained in the CO atmosphere, proved to be much larger than those of similar materials synthesized in the air atmosphere (Fig. 4). We would like to note that in the presence of CO, the type of the reducing agent and the reduction conditions had practically no effect on either the crystallite size (Table 1) or the ECSA of platinum (Fig. 4). The key influence on the processes of nucleation/growth of metallic NPs in this case is determined not by the nature of the reducing agent, but the adsorption of CO molecules on the growing platinum nuclei.

The catalyst activity in ORR was estimated by the kinetic currents (specific activity J_{sp} , $\text{A m}^{-2}(\text{Pt})$, mass activity J_{mass} , $\text{A g}^{-1}(\text{Pt})$) and half-wave potential $E_{1/2}$ which were determined on the basis of the normalized linear voltammograms (Fig. 5a–c and Table 2) as described in Experimental part.

Specific currents ($\text{A m}^{-2}(\text{Pt})$) at the potential of 0.90 V increase in the FA < $\text{F} \leq \text{HiSPEC} \approx \text{F}_{\text{CO}} \leq \text{FA}_{\text{CO}} \leq \text{EG}_{\text{CO}}$ series. In fact, they are very close for all materials, except for FA-value, where the J_{sp} is three-fold less than for the other samples (Table 2). Mass-activity increases in the order (Table 2): FA < $\text{F} \approx \text{HiSPEC} < \text{EG} < \text{FA}_{\text{CO}} < \text{F}_{\text{CO}} \approx \text{EG}_{\text{CO}}$.

As it has been noted earlier the authors of many publications believe that the specific activity of the platinum NPs surface in ORR depends on the size of NPs which increases with its growth [2,5,8,11–13]. In the case of materials under study, the size effect was not observed. Moreover, the lowest specific activity (Table 2) was recorded for the FA catalyst containing the largest platinum nanoparticles (Table 1, Fig. 2). The reason for the reduced specific activity of the FA catalyst might be explained by a particular form of the platinum nanocrystals, characterized by the predominance of facets that are not catalytically active. Unequal specific activity of different platinum nanocrystal facets in electrochemical reactions is described, for example, in [6], and the effect of the nanocrystals shape on the specific activity in ORR was previously observed in [6,10].

For single-crystal platinum electrodes, the dependence of the CV shape on the type of the facet, on which electrochemical reactions are realized, is well known [42]. Among the catalysts investigated in this study, the specific shape of CV, which differs markedly from that of the other materials, was found only for the FA catalyst (Fig. 3A).

To evaluate the shape of the platinum nanocrystals, the powder X-ray diffraction data analysis approach [10] seems to be rather efficient; it is based on the analysis of the anisotropy parameter values, determined from the ratio of the average crystallite sizes, which were calculated using reflections (111) and (200):

$R_v = D_{100}/D_{111} = \text{FWHM}_{111} * \cos(\theta_{200}) / \text{FWHM}_{200} * \cos(\theta_{111})$. Value $R_v = 0.58$ corresponds to the nanocrystals with the cubic faceting, $R_v = 1.73$ –to the nanocrystals with the octahedral one. Intermediate values of R_v correspond to the intermediate forms of the crystals: a truncated cube, a cuboctahedron, a truncated octahedron [10]. For F_{CO} , FA_{CO} and FA materials high-precision measurements on automatic diffractometer ARL X'TRA were performed, the data were collected in the step mode in the range of 2θ 10–90°, with the step of 0.08° and exposure time of 12 s (Fig. 6). The data analysis of the obtained diffraction patterns was carried out with WinPlotr (Fullprof) package, which allowed us to clearly separate reflections (111), (200) (Fig. 6) and determine FWHM values and θ -values for them (Fig. 6, Table 3). The calculated R_v values, in fact, showed that the crystallites in F_{CO} samples ($R_v = 1.47$) and FA_{CO} ($R_v = 1.34$) are close in the form to the truncated octahedron but in the sample FA ($R_v = 0.78$) they are close to the truncated cube. Unfortunately, the transmission electron microscopic photographs of the samples (Fig. 2g–i) do not allow us to identify clearly the shape of the nanocrystals.

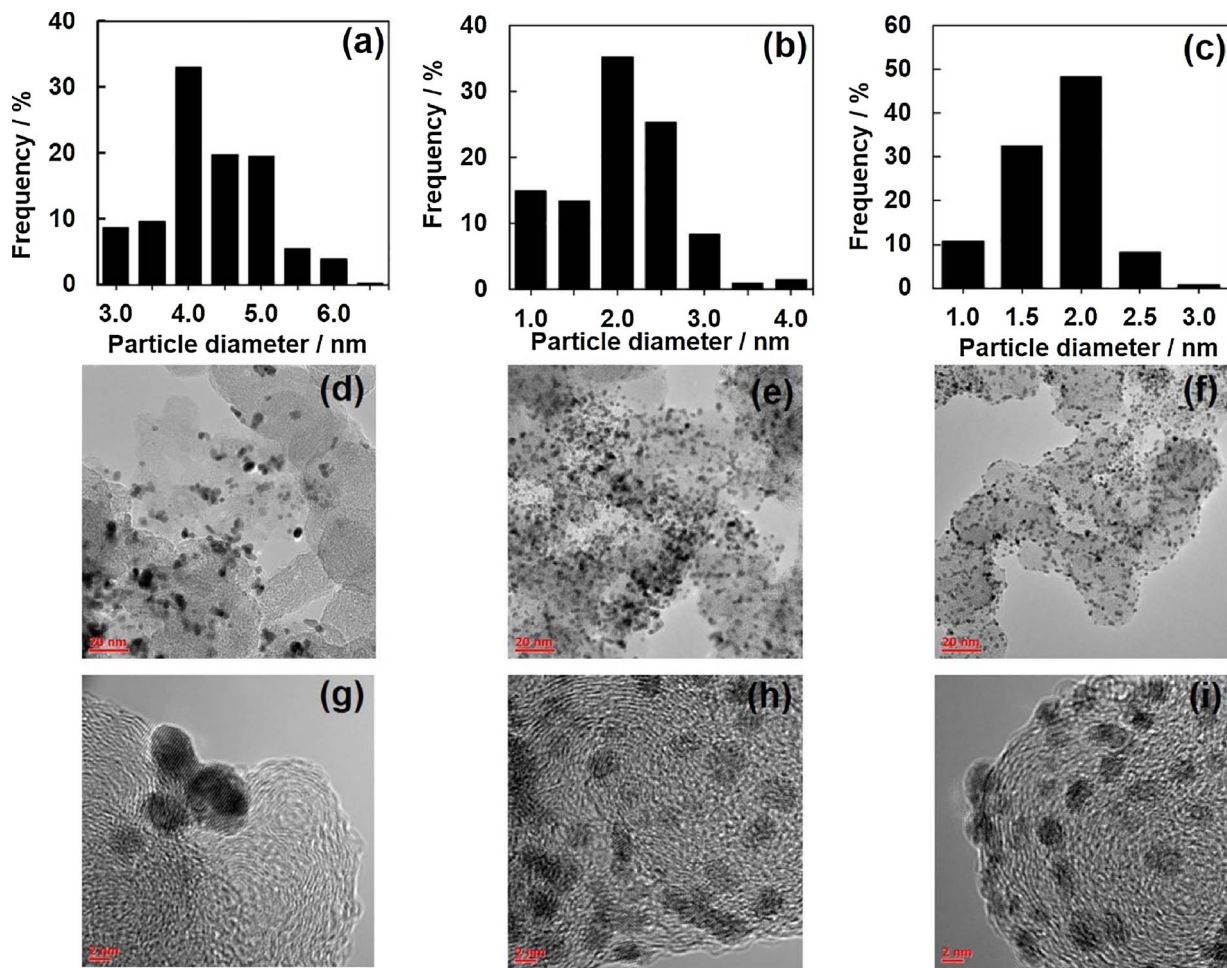


Fig. 2. TEM images for FA (d, g), FA_{CO} (e, h) and EG_{CO} (f, i) samples and corresponding histograms of nanoparticle size distribution (a, b, c).

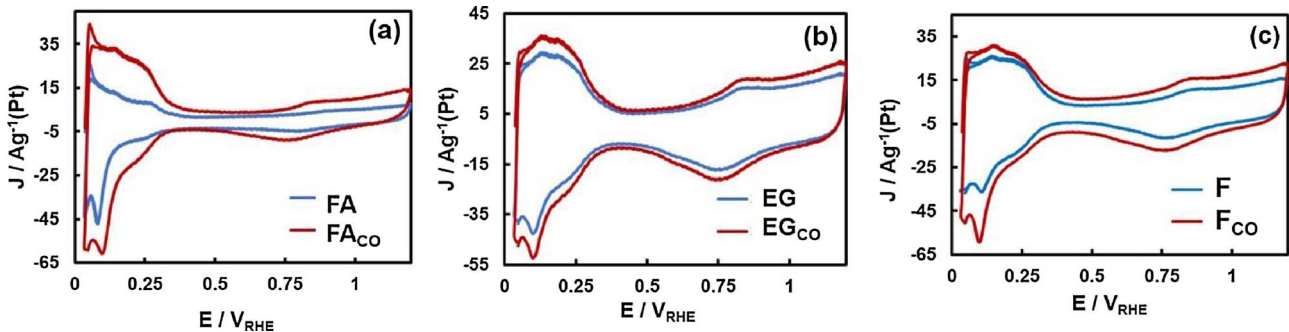


Fig. 3. Cyclic voltammograms (2nd cycle) in an Ar-saturated 0.1 M HClO₄ solution at a scan rate of 20 mV s⁻¹ for Pt/C samples obtained with FA (a), EG (b), and F (c). The samples obtained in the air atmosphere are marked as blue lines, in the CO atmosphere – as red lines. (For interpretation of the references to colour in this figure legend, the reader is referred to the web version of this article.)

Mass activity of the catalysts, determined by the shape of the crystallites, specific activity and the ECSA, increases in the series: FA < < F ≈ HiSPEC < EG ≈ FA_{CO} ≈ F_{CO} ≈ EG_{CO} (Table 2). Moreover, all materials obtained in the CO atmosphere have a higher mass activity compared to analogous samples synthesized in the air atmosphere and the commercial electrocatalyst (Table 2). Higher values for these catalysts also have a half-wave potential (Table 2). On all investigated electrocatalysts, ORR is realized by the four-electron mechanism, typical for platinum: the calculated number of electrons is in the range from 4 to 4.4.

It should be noted that the electrochemical characteristics of the samples obtained in CO atmosphere are very close (Table 2). For

example, their mass activity in ORR ranges from 121 to 126 A g⁻¹(Pt), and the specific activity is 0.87–0.89 A m⁻²(Pt) (Table 2). A half-wave potential has almost the same value (0.93–0.94 V).

The obtained results allow us to make the conclusion: the type of the gas atmosphere, namely, the presence of CO molecules, has a decisive influence on the structural and morphological characteristics of Pt/C catalysts synthesized in the liquid-phase. When the synthesis is performed in the air atmosphere (no CO-flow is injected into the solution), the size and the structure of the formed platinum nanoparticles depend on the type of the reducing agent and the conditions of the liquid-phase synthesis (medium composition, pH, temperature). However, in the presence of CO molecules, these molecules displace other types of

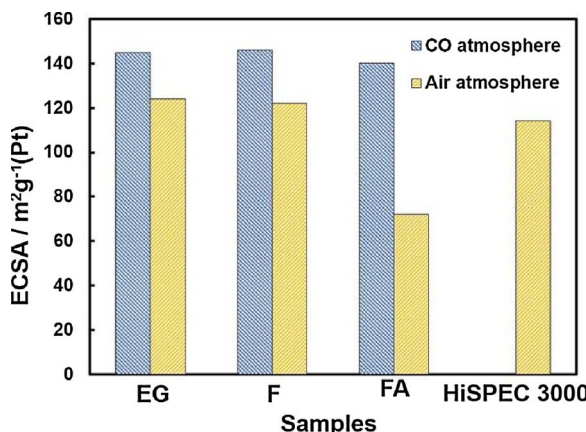


Fig. 4. ECSA values for the commercial and synthesized Pt/C materials. Yellow columns in the histogram are the samples synthesized in the air atmosphere, the blue ones – in the CO atmosphere. (For interpretation of the references to colour in this figure legend, the reader is referred to the web version of this article.)

adsorbs from the surface of the growing platinum nuclei because of the strong chemisorptive interaction with platinum, thus increasing the activation energy of their growth. Acting as an effective surfactant, they also prevent aggregation of NPs. As a result, Pt/C catalysts are formed. They contain smaller nanoparticles with a narrow size distribution (Table 1, Fig. 2) and, as a consequence, with the high ECSA values. Deposition and fixation of Pt particles at the interface with carbon is slightly difficult too, which leads to a certain decrease in the mass fraction of the metal in the samples. As a result, the catalysts obtained in the CO atmosphere show a higher mass activity in ORR than the analogues synthesized in the air atmosphere.

The strongest effect of CO molecules on the size of platinum nanoparticles formed during the liquid-phase synthesis is observed when formic acid is used as a reducing agent. Therefore, namely for this system, the ability to control NPs size by means of introducing CO into the reaction mixture at various stages of the liquid-phase synthesis was studied. For this reason, the CO-flow was started through the reaction mixture at different times after the start of the synthesis: after 0 (from the very beginning), 5, 10, 20, 30 and 60 min (in fact, at the end of the process). For Pt/C catalysts containing 15–17 wt% of Pt, the average size of Pt NPs and ECSA, calculated by the cyclic voltammetry data (Fig. 7) was determined, as described in Experimental section. The results of the measurements are shown in Fig. 8.

Indeed, the CO-flow clearly “freezes” nucleation-growth processes of the platinum nuclei. In addition to the obvious confirmation of the ability to control the NPs size and, as a consequence, the ECSA value, the obtained results (Fig. 8) provide valuable information on the kinetics of the platinum nuclei formation: nucleation of NPs occurs during the first 4 min of the synthesis, and subsequent intensive growth practically ends in 11 min after the beginning of the synthesis. This evidence

Table 2

The ORR parameters were determined for $E = 0.90$ V_{RHE}.

Sample	J , mA	J_{mass} , A g ⁻¹ (Pt)	J_{sp} , A m ⁻² (Pt)	$E_{1/2}$, V _{RHE} (1600 rpm)
EG	0.72	117 ± 6	0.94 ± 0.05	0.92
EG _{CO}	0.74	126 ± 6	0.87 ± 0.04	0.94
F	0.69	94 ± 5	0.77 ± 0.04	0.88
F _{CO}	0.73	125 ± 6	0.85 ± 0.04	0.94
FA	0.37	22 ± 2	0.31 ± 0.03	0.81
FA _{CO}	0.72	121 ± 6	0.89 ± 0.05	0.93
HiSPEC 3000	0.67	96 ± 5	0.84 ± 0.04	0.89

is confirmed by a sharp change in values of D_{Av} and the ECSA in the time range of the “inhibitory agent” injection from about 4–11 min after the synthesis has been started (Fig. 8).

4. Conclusions

Control over the Pt/C catalysts structure under synthesis (the size of Pt nanoparticles, their spatial and size distribution) is of great importance, as it helps to increase their mass activity, when used in PEMFC and DMFC, and consequently, to reduce Pt-loading in catalyst layers in membrane-electrode assembly.

In this study platinum-carbon catalysts with Pt loading from 15.2 to 17.3% wt. were obtained by the liquid-phase synthesis. Ethylene glycol, formaldehyde and formic acid were used as reducing agents. The synthesis was carried out both at ambient conditions (air atmosphere) and in the presence of carbon monoxide (CO-saturated solvent, CO atmosphere).

The novel, and most exciting result of the study performed is that transmission of CO, which is well known to be a catalytic poison, makes such a strong and helpful impact on the process of Pt nanoparticles nucleation/growth, that the nature of the reducing agent as well as synthesis conditions lose their primary importance. The catalysts obtained in the CO atmosphere have larger ECSA (140 – 146 m² g⁻¹ of Pt) compared to analogues synthesized in the air atmosphere (72 – 120 m² g⁻¹ of Pt) due to the small NPs platinum size, as well as their narrow size distribution. Unlike materials synthesized in the air atmosphere, the ECSA values of the catalysts obtained in the CO atmosphere are practically independent of the nature of the reducing agent and other synthesis conditions. The same catalysts exhibit the highest mass activity values in ORRs, superior to those synthesized in the air atmosphere, as well as the commercial Pt/C catalyst HiSPEC 3000 (20% wt. of Pt).

The CO effect on the microstructure of the catalyst is caused by the size-dependent chemisorption of its molecules on the surface of the growing platinum nuclei. This chemisorptive shell increases the activation energy of the nucleation growth to a greater extent than the activation energy of nucleation, which results in the decrease in the average size of the nanoparticles. The nanoparticle shells, formed from

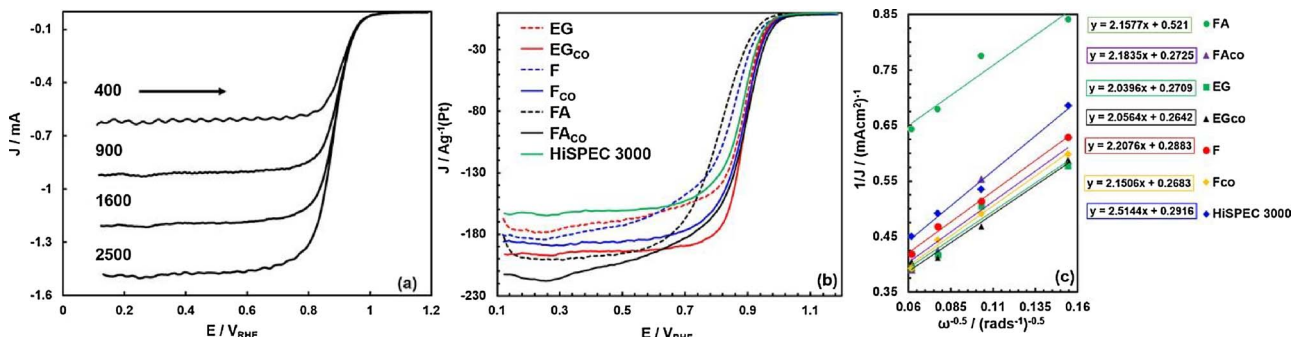


Fig. 5. Voltammograms with the linear potential sweep (a) at different rotation speeds of the disk electrode for the EG_{CO} sample; (b) for the synthesized Pt/C samples and commercial catalyst HiSPEC 3000 at the rotation speed 1600 rpm and (c) corresponding to Koutecky-Levich plots for studied samples. O₂-saturated 0.1 M HClO₄ solution; scan rate – 20 mV s⁻¹.

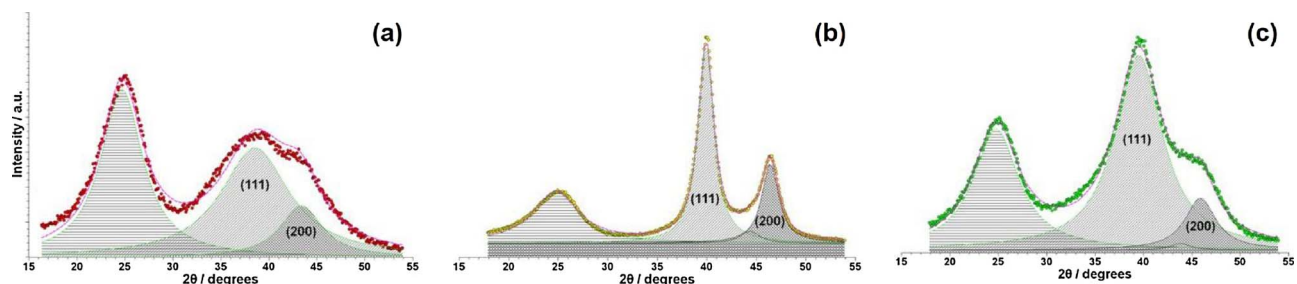


Fig. 6. Schemes of powder X-ray diffraction patterns analysis for FCo (A), FA (B), FAcO (C) samples.

Table 3
Main parameters obtained from the powder X-ray diffraction data.

Sample	Pt (111)		Pt (200)		R_v
	2θ, degrees	FWHM, degrees	2θ, degrees	FWHM, degrees	
FCo	38.1	9.8	43.2	6.6	1.47
FA	40.0	1.9	46.3	2.4	0.78
FA _{CO}	39.5	6.0	45.8	4.4	1.34

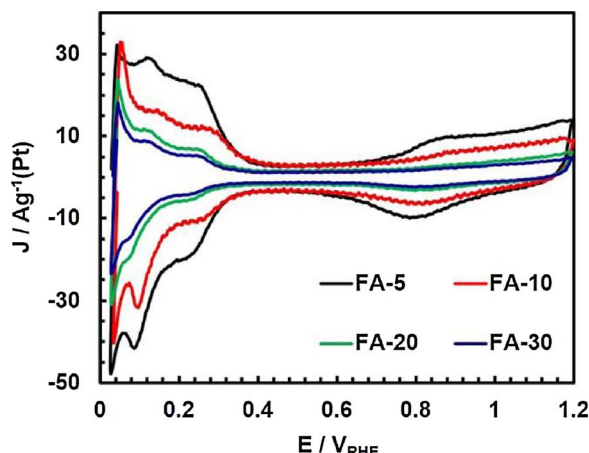


Fig. 7. Cyclic voltammograms (2nd cycle) of Pt/C catalyst samples obtained by reduction of Pt (IV) with formic acid. Ar-saturated 0.1 M HClO₄; scan rate – 20 mV s⁻¹. The time elapsed from the onset of the synthesis to the onset of CO-flow via the solvent: FA-5 – 5 min, FA-10 – 10 min, FA-20 – 20 min, FA-30 – 30 min.

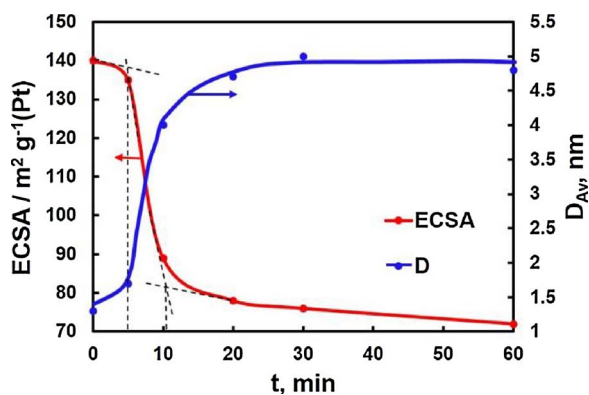


Fig. 8. Dependence of the average size of platinum crystallites and ECSA for Pt/C catalysts on the time elapsed from the onset of the synthesis to the onset of the CO-flow. The reducing agent is formic acid.

the carbon monoxide molecules, hinder their agglomeration and insignificantly impede the absorption of NPs on the surface of the carbon carrier. As a result, the mass fraction of platinum in the catalyst decreases slightly, the ECSA is significantly increased and, as a

consequence, the mass activity of the catalysts in ORR is increased too. Solvent molecules and other particles, initially present in the reaction medium or formed during the reaction, are not able to compete with CO molecules as an adsorbent and, in the presence of CO, have almost no effect on the growth of the platinum nuclei.

It has been found that when formic acid is used as a reducing agent in the liquid-phase synthesis, relatively large platinum NPs (~4.3 nm) are formed and their specific activity in ORR is significantly lower, compared to all other materials that were studied. Apparently, platinum nanocrystals, formed upon the reduction with Pt (IV) formic acid, have the shape of a cube (truncated cube) and contain a much higher fraction of facets with less catalytic activity in ORR than nanocrystals of the octahedral form, produced by other reducing agents or in the presence of CO molecules.

The liquid phase synthesis in formic acid taken as an example has shown that the injection of CO molecules into the reaction medium at different time-points of the synthesis could be used to control the size of the formed platinum nanoparticles. It has been established that an intensive growth of platinum nanoparticles in this case occurs in a narrow time range (from the 4th to the 11th minute from the beginning of the synthesis). This successfully tested approach is a good chance to study the kinetic regularities of nucleation/growth of platinum nuclei in the liquid phase.

Thus, the present study demonstrates a simple, universal and reasonable way to control the structure of Pt/C catalysts during their liquid phase synthesis. The Pt/C catalysts obtained in the CO atmosphere possess higher ECSA and, as a result, higher mass activity in the ORR compared to Pt/C analogues obtained in ambient conditions. At the end of the synthesis, the CO molecules are easily removed from the surface of Pt nanoparticles and a carbon carrier with the help of the standard methods for washing and drying the synthesized materials.

Author contributions

Electrochemical experiments were designed and performed by Anastasia Alekseenko, Evgenia Ashihina and Svetlana Shpanko. XRD measurements were performed and interpreted by Vadim Volochaev. The results of TEM study and a part of electrochemical measurements were interpreted by Vladimir Guterman, who assisted with the electrochemical measurements. The catalyst was synthesized and chemically characterized by Anastasya Alekseenko. The manuscript was written by Vladimir Guterman, Svetlana Shpanko and Olga Safronenko. All authors contributed to scientific discussions and assisted with the writing of the manuscript.

Notes

The authors declare no competing financial interest.

Acknowledgments

This research was supported by the Ministry of Education and Science of the Russian Federation (project № 13.3005.2017/4.6). The

TEM study of the catalysts was carried out in «Systems for microscopy and analysis» Ltd., Moscow.

Appendix A. Supplementary data

Supplementary data associated with this article can be found, in the online version, at <https://doi.org/10.1016/j.apcath.2018.01.013>.

References

- [1] R.P. O'Hare, S.W. Cha, W.M. Colella, F.B. Prinz, *Fuel Cell Fundamentals*, 2nd ed., Wiley, New York, 2009, p. 576.
- [2] D. Thompsett, *Catalysts for the proton exchange membrane fuel cell*, in: W. Vielstich, A. Lamm, H.A. Gasteiger (Eds.), *Handbook of Fuel Cells. Fundamentals, Technology and Applications*, 3 Wiley & Sons Ltd, New York, 2003, pp. 6–23.
- [3] D.W.H. Banham, S. Ye, *ACS Energy Lett.* (2017), <http://dx.doi.org/10.1021/acsenergylett.6b00644>.
- [4] A.B. Yaroslavtsev, Yu. A. Dobrovolsky, N.S. Shaglaeva, L.A. Frolova, E.V. Gerasimova, E.A. Sanginov, *Russ. Chem. Rev.* 81 (2012) 191–220, <http://dx.doi.org/10.1070/RC2012v081n03ABEH004290>.
- [5] Sh. Sui, X. Wang, Su Y. Zhou, S. Riffat, Ch. Liu, *J. Mater. Chem. A* 5 (2017) 1808–1825, <http://dx.doi.org/10.1039/C6TA08580F>.
- [6] M. Cao, D. Wu, R. Cao, *ChemCatChem* 6 (2014) 26–45, <http://dx.doi.org/10.1002/cctc.201300647>.
- [7] Z.W. She, J. Kibsgaard, C.F. Dickens, I. Chorkendorff, J.K. Nørskov, T.F. Jaramillo, *Science* 146 (2017) 355, <http://dx.doi.org/10.1126/science.aad4998>.
- [8] J.C. Meier, C. Galeano, I. Katsounaros, J. Witte, H.J. Bongard, A.A. Topalov, C. Baldizzone, S. Mezzavilla, F. Schüth, K.J.J. Mayrhofer, *Beilstein J. Nanotechnol.* 5 (2014) 44–67, <http://dx.doi.org/10.3762/bjnano.5.5>.
- [9] A.A. Alekseenko, V.E. Guterman, V.A. Volochaeve, S.V. Belenov, *Inorg. Mater.* 51 (2015) 1258–1263, <http://dx.doi.org/10.1134/S0020168515120018>.
- [10] I.N. Leontyev, S.V. Belenov, V.E. Guterman, P. Haggi-Ashtiani, A.P. Shaganov, B.J. Dkhil, *Phys. Chem. C* 115 (2011) 5429–5434, <http://dx.doi.org/10.1021/jp1109477>.
- [11] H.A. Gasteiger, S.S. Kocha, B. Sompalli, F.T. Wagner, *Appl. Catal. B* 56 (2005) 9–35, <http://dx.doi.org/10.1016/j.apcath.2004.06.021>.
- [12] D. Li, C. Wang, D.S. Strmcnik, D.V. Tripkovic, X. Sun, Y. Kang, M. Chi, J.D. Snyder, D. Van Der Vliet, Y. Tsai, V.R. Stamenkovic, S. Sun, N.M. Markovic, *Energy Environ. Sci.* 7 (2014) 4061–4069, <http://dx.doi.org/10.1039/C4EE01564A>.
- [13] Yu. Deng, G.K.H. Wiberg, A. Zana, Sh. Sun, M. Arenz, *ACS Catal.* 7 (2017) 1–6, <http://dx.doi.org/10.1021/acscatal.6b01534>.
- [14] V.E. Guterman, S.V. Belenov, A.A. Alekseenko, N. Yu. Tabachkova, V.A. Volochaeve, *Russ. J. Electrochem.* 53 (2017) 531–539, <http://dx.doi.org/10.1134/S1023193517050081>.
- [15] V.I. Pavlov, E.V. Gerasimova, E.V. Zolotukhina, G.M. Don, Yu.A. Dobrovolsky, A.B. Yaroslavtsev, *Nanotechnol. Russ.* 11 (2016) 743–750, <http://dx.doi.org/10.1134/S199507801606015X>.
- [16] E. Antolini, *Appl. Catal. B* 88 (2009) 1–24, <http://dx.doi.org/10.1016/j.apcath.2008.09.030>.
- [17] Y.-J. Wang, N. Zhao, B. Fang, H. Li, X.T. Bi, H. Wang, *Chem. Rev.* 115 (2015) 3433–3467, <http://dx.doi.org/10.1021/cr500519c>.
- [18] V.V. Pryadchenko, V.V. Srabionyan, S.V. Belenov, V.A. Volochaeve, A.A. Kurzin, L.A. Avakyan, I. Zizak, V.E. Guterman, L.A. Bugaev, *Appl. Catal. A* 525 (2016) 226–236, <http://dx.doi.org/10.1134/S1995078017020033>.
- [19] V.E. Guterman, S.V. Belenov, A. Yu. Yu. Pakharev, M. Min, N. Yu. Tabachkova, E.B. Mikheykina, L.L. Vysochina, T.A. Lastovina, *Int. J. Hydrogen Energy* 41 (2016) 1609–1626, <http://dx.doi.org/10.1016/j.ijhydene.2015.11.002>.
- [20] A. Marcu, G. Toth, R. Srivastava, P. Strasser, *J. Power Sources* 208 (2012) 288–295, <http://dx.doi.org/10.1016/j.jpowsour.2012.02.065>.
- [21] D.H. Jung, S.J. Bae, S.J. Kim, K.S. Nahm, P. Kim, *Int. J. Hydrogen Energy* 36 (2011) 9115–9122, <http://dx.doi.org/10.1016/j.ijhydene.2011.04.166>.
- [22] P.C. Favilla, J.J. Acosta, C.E. Schvezov, D.J. Sercovich, J.R. Collet-Lacoste, *Chem. Eng. Sci.* 101 (2013) 27–34, <http://dx.doi.org/10.1016/j.ces.2013.05.067>.
- [23] H.A. Huy, T.V. Man, H.T. Tai, V.T.T. Ho, *Sci. Tech.* 53 (2016) 472–482, <http://dx.doi.org/10.15625/0866-708X/54/4/7308>.
- [24] Z. Zhou, W. Zhou, S. Wang, G. Wang, L. Jiang, H. Li, G. Sun, Q. Xin, *Catal. Today* 93–95 (2004) 523–528, <http://dx.doi.org/10.1016/j.cattod.2004.06.121>.
- [25] V.E. Guterman, S.V. Belenov, O.V. Dymnikova, T.A. Lastovina, Ya. B. Konstantinova, N.V. Prutsakova, *Inorg. Mater.* 45 (2009) 498–505, <http://dx.doi.org/10.1134/S0020168509050082>.
- [26] V.E. Guterman, A.Y. Pakharev, N.Y. Tabachkova, *Appl. Catal. A* 453 (2013) 113–120, <http://dx.doi.org/10.1016/j.apcata.2012.11.041>.
- [27] C. Coutanceau, S.T.W. Baranton Napporn, A.A. Hashim (Ed.), *In The Delivery of Nanoparticles*, InTech, 2012, pp. 403–431.
- [28] H. Bönnemann, W. Brijoux, R. Brinkmann, E. Dinjus, T. Joussen, B. Korall, *Angew. Chem. Int. Engl.* 30 (1991) 1312–1314, <http://dx.doi.org/10.1002/anie.199113121>.
- [29] J. Lemus, J. Bedia, L. Calvo, I.L. Simakova, D. Yu. Murzil;1;1;n, B.J.M. Etzold, J.J. Rodrigues, M.A. Gilarranz, *Catal. Sci. Technol.* 6 (2016) 5196–5206, <http://dx.doi.org/10.1039/C6CY00403B>.
- [30] Y. Kang, M. Li, Y. Cai, M. Cargnello, R.E. Diaz, Th. R. Gordon, N.L. Wieder, R.R. Adzic, R.J.J. Gorte, *Am. Chem. Soc.* 135 (2013) 2741–2747, <http://dx.doi.org/10.1021/ja3116839>.
- [31] L. Kacenauskaita, J. Quinson, H. Schultz, J.J.K. Kirkensgaard, S. Kunz, T. Vosch, M.J. Arenz, *ChemNanoMat* 3 (2017) 89–93, <http://dx.doi.org/10.1002/cnma.201600313>.
- [32] Tiankai Chenand, Jianping Xie, *Chem. Rec.* 16 (2016) 1761–1771, <http://dx.doi.org/10.1002/ctr.201600004>.
- [33] Yijin Kang, Xingchen Ye, Christopher B. Murray, *Angew. Chem. Int. Ed.* 49 (2010) 6156–6159, <http://dx.doi.org/10.1002/anie.201003383>.
- [34] Chunhua Cui, Lin Gan, Maximilian Neumann, Marc Heggen, Roldan Cuenya, Peter Strasser, *J. Am. Chem. Soc.* 136 (2014) 4813–4816, <http://dx.doi.org/10.1021/ja4124658>.
- [35] V.E. Guterman, A.A. Alekseenko, V.A. Volochaeve, N. Yu. Tabachkova, *Inorg. Mater.* 52 (2016) 23–28, <http://dx.doi.org/10.1134/S002016851601009X>.
- [36] A.A. Alekseenko, V.E. Guterman, N.Y. Tabachkova, O.I. Safronenko, *J. Solid State Electrochem.* 21 (2017) 2899–2907, <http://dx.doi.org/10.1007/s10008-017-3581-8>.
- [37] S.A. Kirakosyan, A.A. Alekseenko, V.E. Guterman, V.A. Volochaeve, N. Yu. Tabachkova, *Nanotechnol. Russ.* 11 (2016) 287–296, <http://dx.doi.org/10.1134/S1995078016030095>.
- [38] K. Shinozaki, J.W. Zack, S. Pylypenko, B.S. Pivovar, S.S. Kocha, *J. Electrochem Soc.* 162 (2015) F1384–F1396, <http://dx.doi.org/10.1149/2.0551512jes>.
- [39] D. Vliet, D.S. Strmcnik, Ch. Wang, V.R. Stamenkovic, N.M. Markovic, M.T.M. Kope, *J. Electroanal. Chem.* 647 (2010) 29–34, <http://dx.doi.org/10.1016/j.jelechem.2010.05.016>.
- [40] W.J. Khudhayer, N.N. Kariuki, X. Wang, D.J. Myers, A.U. Shaikh, T. Karabacak, *J. Electrochem. Soc.* 158 (2011) B1029–B1041, <http://dx.doi.org/10.1149/1.359901>.
- [41] H. Oh, J. Oh, Y. Hong, H. Kim, *Electrochim. Acta* 52 (2007) 7278–7285, <http://dx.doi.org/10.1016/j.electacta.2007.05.080>.
- [42] S.J. Mukerjee, *Appl. Electrochem.* 20 (1990) 537–548, <http://dx.doi.org/10.1007/BF01008861>.